

Published in final edited form as:

Technology (Singap World Sci). 2013 October 2; 1(1): 49–. doi:10.1142/S2339547813500040.

Measuring neutrophil speed and directionality during chemotaxis, directly from a droplet of whole blood

Anh N. Hoang^{1,*}, Caroline N. Jones^{2,*}, Laurie Dimisko¹, Bashar Hamza¹, Joseph Martel³, Nikola Kojic¹, and Daniel Irimia²

¹The BioMEMS Resource Center, Department of Surgery, Massachusetts General Hospital, Boston, USA

²The BioMEMS Resource Center, Department of Surgery, Massachusetts General Hospital, Harvard Medical School, Shriners Burns Hospital, Boston, USA

³The BioMEMS Resource Center, Department of Surgery, Massachusetts General Hospital, Harvard University School of Engineering and Applied Sciences, Boston, USA

Abstract

Neutrophil chemotaxis is critical for defense against infections and its alterations could lead to chronic inflammation and tissue injury. The central role that transient alterations of neutrophil chemotaxis could have on patient outcomes calls for its quantification in the clinic. However, current methods for measuring neutrophil chemotaxis require large volumes of blood and are time consuming. To address the need for rapid and robust assays, we designed a microfluidic device that measures neutrophil chemotaxis directly from a single droplet of blood. We validated the assay by comparing neutrophil chemotaxis from finger prick, venous blood and purified neutrophil samples. We found consistent average velocity of ($19 \pm 6 \mu\text{m}/\text{min}$) and directionality (91.1%) between the three sources. We quantified the variability in neutrophil chemotaxis between healthy donors and found no significant changes over time. We also validated the device in the clinic and documented temporary chemotaxis deficiencies after burn injuries.

INNOVATION

Traditional neutrophil chemotaxis assays require careful steps of neutrophil isolation to avoid artifacts from inappropriate activation of neutrophils. More recently, microfluidic assays have integrated the neutrophil isolation on the chip, however, the use of adhesion molecules to selectively capture neutrophils to the migration surfaces is also prone to activation artifacts. In this assay, we circumvent the need for neutrophil separation by using whole blood directly in conjunction with microchannels with precise geometry and neutrophil-specific chemoattractants. Specifically, we implement right angle turns to stop the granular-flow of blood through migration channels with cross section larger than that of red blood cells, while allowing active neutrophil migration.

INTRODUCTION

Neutrophils represent the dominant population of white blood cells in circulation and the first responders to bacterial and fungal infections. Neutrophils are also involved in various chronic and acute inflammatory conditions ranging from atherosclerosis¹ to burn injury². For their major contribution to health and disease conditions, the absolute neutrophil count (ANC) is part of the standard cell blood analysis in clinical laboratories. Both neutropenia (less than 1500 neutrophils per microliter of blood) and neutrophilia (> 7000/ μ L) require additional clinical investigation whenever detected³. However, despite being one of the most ubiquitous tests, the value of neutrophil count in the diagnosis of infection and sepsis is increasingly questioned. One issue is the implicit assumption that all neutrophils in the blood are fully functional⁴. For the majority of healthy individuals this premise is true. Permanent neutrophil dysfunctions are extremely rare and only ~20 people/year in the US are diagnosed with such diseases (e.g. chronic granulomatous disease, Shwachman-Diamond syndrome, leukocyte adhesion deficiency, myeloperoxidase deficiency etc⁵⁻⁸). However, temporary alterations of neutrophil functionality are far more frequent and largely overlooked in the clinic. Neutrophil chemotaxis impairment has been described in various conditions associated with higher incidence of infections, including burn and trauma injuries^{2,9}, major surgery¹⁰, diabetes when poorly controlled¹¹, periodontal disease^{12,13}, viral infections e.g. influenza¹⁴, cytomegalovirus¹⁵, HIV^{16,17}, bacterial infections e.g. tuberculosis¹⁸, cholera¹⁹, and tropical diseases e.g. malaria²⁰. Several drugs have been shown to decrease neutrophil chemotaxis including chemotherapy²¹, anti-hypertensives²², anesthetics^{23,24}, antacids²⁵, antifungal agents²⁶ etc. Of all neutrophil functions, chemotaxis, the ability to move directionally towards a source of chemoattractant appears to be one of the most sensitive to perturbations. Chemotaxis is the last function acquired by neutrophils maturing in the bone marrow before release²⁷, and is the first to be significantly altered during various diseases. Chemotaxis can be altered days before changes could be measured in the ability of neutrophils to phagocytose, produce reactive oxygen species, or release of lytic enzymes.

Identifying the alterations of neutrophil chemotaxis early could help estimate the risk for infections more accurately. However, existing assays to measure neutrophil migration are often inadequate for routine clinical laboratories, and are confined mostly to research laboratories. Several factors contribute to this situation, including the requirement for the assay to be performed quickly, within hours after the blood draw, the use of large volumes of blood, the time consuming and cumbersome neutrophil isolation techniques. Moreover, traditional migration assays (transwell assay, Dunn chamber, micropipette assay) lack accuracy in detecting chemotaxis changes in the absence of pre-disease or pre-treatment controls. Most microfluidic devices that have the precision and accuracy to measure neutrophil chemotactic function require specialized training.

To address the need for a neutrophil functional assay that is rapid, robust, user-friendly, and requiring minimal blood volume, we have developed a microfluidic device that measures neutrophil chemotaxis directly from a small droplet of whole blood. The device is simple to operate and allows for highly reproducible measurements of neutrophil speed and

directionality with no sample processing and neutrophil isolation procedures on or off the chip.

RESULTS

Platform design, characterization and modeling

In the doughnut shaped device, which is completely submerged in cell culture media, chemoattractant gradients were established by diffusion in the absence of convection between an array of 16 chemokine reservoirs (focal chemoattractant chambers - FCCs) and one central whole blood loading chamber (WBLC) (Fig. 1a,b). To selectively allow neutrophils to migrate towards the chemotactic gradient inside the device while preventing red blood cells (RBCs) from blocking the channels, we incorporated an RBC filtration comb between the WBLC and migration channels. To quantify the directionality, or the ability of migrating neutrophils to correctly follow a chemoattractant gradient, we incorporated a bifurcation between a channel leading to the focal chemotactic chamber and a channel exiting the device. Finally, we quantified the accumulation of neutrophils (blue) in the FCC by counting the neutrophils arriving over-time.

Biophysical modeling of chemoattractant diffusion shows that chemoattractant gradients along the migration channel to the FCC decrease by < 5% by the end (200 min) of the experiment (Fig. 1c). To confirm the dynamics and stability of the chemoattractant gradient predicted to be found between the FCC and the WBLC, we primed the device with fluorescein (molecular mass, 376 Da) and measured the fluorescence levels over time. Linear gradients of chemoattractant were formed along migration channels and lasted for more than 200 min after priming the FCCs with the chemoattractant, matching the predictions of a biophysical model (Fig. 1d).

Red blood cell filter optimization

One practical issue related to the use of whole blood in the device was to identify effective designs to avoid the blocking of the neutrophil migration paths by RBCs. In spite of the absence of fluid flow, blood cells in the WBLC impinge on each other, pushing some of the cells through the migration channel. Over the course of experiment, significant numbers of mostly RBCs could fill a straight channel from the loading chamber to the outer compartment. This “granular flow” of RBCs can potentially alter the chemokine gradients from the chemokine reservoirs and obstruct the migration path of the neutrophils. To limit the entrance of RBCs, one strategy could be to use channels with cross sections smaller than that of RBCs. However, such channels could be completely obstructed by RBCs at their entrance, precluding the formation of gradients. Smaller cross sectional areas of the migration channel could also impede neutrophil migration. Our method for preventing RBCs from advancing into the migration channels was to block them inside channels with cross sections larger than the size of RBCs.

To accomplish effective RBC blocking, while allowing large enough spaces for neutrophils to move without restriction, we used a filtration comb with 90° turns, close to the entrance. For this, we designed migration channels that have a height (3 μm) less than the diameter of

the RBC (7 μm), ensuring a side orientation of RBCs entering the channels. The channels were wider than the RBCs and RBC blocking was achieved at 90° turns in the channels (Fig. 2).

To optimize our comb design and understand how a group of RBCs move through various microchannels, we employed a computational 2-D finite-element model, building on our previous numerical platform^{28,29}. The model is based on strong solid-fluid coupling, which allows the incorporation of deformable solid bodies (i.e. RBCs) in fluid-filled channels. We simulated the granular flow of RBCs through small channels and applied a force equivalent to the apparent weight in media of a stack of 12 RBCs. We focused specifically on how a group of 10 RBCs that have entered the microchannels from the main reservoir of the device, traverse a 90° turn in channels with three different widths (9, 12, and 14 μm). The initial RBC configuration of 10 RBCs (each with a diameter of 7.5 μm) in the entrance segment of the channel was random and identical for all the simulations (Fig. 2a). The results show that as soon as one RBC is pushed into the corner, it blocks the advance of all RBCs behind it by restricting the cross section of the channel to less than one RBC diameter. This strategy works because the granular flow force pushing cells in the channel is not enough to deform them through the restricted section. The results show that reaching a stable configuration is less likely in larger channels when progressively more and more RBCs traverse the corner as the channel width increases (Fig. 2b–d). Based on the model simulations, we chose a 12 μm width for the channels and a “comb” design that consists of multiple channels in parallel and right angle turns, for the entrance to the migration channels.

The comb design proved more efficient in blocking the entrance of RBCs in the migration channels compared to the straight channels (Fig. 2e,f). RBC contamination is reduced by 63.4% in the FCC and totally eliminated at the migration channel exit (Fig. 2f). Detailed time-lapse images of the comb section of the device show that neutrophils are able to actively migrate past the RBCs in the filtration comb without perturbations in cell motility speed or directionality (Fig. 2g).

Assay validation with finger prick and venous healthy donor blood sources

We validated the whole blood device assay by loading whole blood from finger prick and venous sources, as well as isolated neutrophils toward fMLP, a standard chemoattractant. Neutrophils from the two whole blood sources, as well as isolated neutrophils, began migrating towards the fMLP [100 nM] gradient within 20 minutes and neutrophil accumulation numbers from all three sources were consistent around 135 ± 20 cells/device after 3.5 hours (P-value < 0.001, $R^2 = 0.98$) (Fig. 3a). The rate of neutrophil accumulation remained constant for the length of the 200 min experiment in all blood sources. We observed higher variability of neutrophil counts with the finger prick blood source compared to the venous or isolated neutrophil sources (Fig. 3a), which may reflect higher heterogeneity of the neutrophil population in the capillaries compared to the whole blood. We then measured variability between healthy donor neutrophil migration from whole blood finger source towards fMLP [100 nM]. Of interest, for 5 out of 7 donors neutrophil migration counts clustered tightly around the average of 92 ± 35 cells after 200 min.

However, two donors had significantly higher neutrophil migration counts, which may be representative of the variation in innate immune response in the human population (Fig. 3b). To determine device-device variation, we loaded whole blood from a finger prick of a healthy donor into 6 separate devices and quantified neutrophil accumulation to a gradient of fMLP [100 nM] (Fig. 3c). The device-device variation was 14.1% (83 ± 12 cells after 200 min), over the duration of the experiment. Finally, we established a healthy donor baseline, measuring neutrophil accumulation from finger prick whole blood from the same healthy donor at 1 week intervals for a total of 3 weeks. The experiment yielded equivalent neutrophil accumulation values, thus suggesting high experimental reproducibility as well as a consistent accumulation baseline for the same volunteer (Fig. 3d). The confirmation of a consistent baseline of neutrophil recruitment in a healthy volunteer, suggests that perturbations in this baseline could represent significant clinical changes in the innate immune response, such as injury, infection or dysfunction that would be useful in diagnosis or predictions of future clinical outcomes.

Neutrophil chemotaxis towards standard chemoattractants

Neutrophil recruitment toward both fMLP and LTB₄ demonstrated dose-dependent chemotactic responses. Neutrophil migration at three different chemoattractant concentrations (10 nM, 50 nM, or 100 nM) was examined. Overall, increased cell migration was observed at higher concentration. Maximal cell recruitment was observed at the 100 nM concentration in the FCC (Fig. 4a). A concentration of 100 nM was therefore used for all burn patient samples in subsequent experiments. A gradient of fMLP [100 nM] recruited neutrophils from finger pick whole blood at a two-fold higher count (86 ± 7 cells/device after 200 min) than LTB₄ (39 ± 12 cells/device after 200 min) (Fig. 4a). This trend differs from our previous studies on isolated neutrophils³⁰, where LTB₄ was shown to be a more potent chemoattractant for neutrophils than fMLP (25% increase in neutrophil recruitment). This discrepancy between isolated neutrophils and neutrophils in whole blood indicates that factors in healthy whole blood serum can suppress the migration of neutrophils towards LTB₄, an important mediator in inflammation. It also indicates that for accurate measurements of neutrophil function reflecting the situation in the body, assays should include serum^{31,32}. Neutrophil velocity from finger prick whole blood was comparable for both fMLP (19 ± 6 $\mu\text{m}/\text{min}$) and LTB₄ (20 ± 7 $\mu\text{m}/\text{min}$) (Fig. 4b). Neutrophil velocities were also consistent between venous whole blood and finger prick whole blood for both fMLP and LTB₄ chemoattractants (Fig. 4b). The bifurcation in the device design allows for the quantification of neutrophils directionality by comparing the number of cells that migrated towards the chemoattractant gradient from the FCC to the number of cells that become “lost” and exit the device. This directional index is clinically relevant as it provides a quantitative measurement for correct neutrophil response to a site of injury or infection. The “lost” or non-directional neutrophils would potentially migrate and cause unnecessary damage to healthy tissue or organs. Neutrophils from finger prick and venous healthy donor whole blood sources have a directionality index greater than 0.9 for both fMLP and LTB₄ (Fig. 4c). In our assay, the inclusion of fibronectin promotes neutrophil adherence³³ and acts as a blocking agent (in addition to 0.2% human serum albumin) for the glass surface of the device and does not appear to change final neutrophil counts migrating towards fMLP (Fig. 4d).

Dysfunction in neutrophil recruitment after burn in human patient

We utilized the novel whole blood device to monitor neutrophil chemotaxis function in a patient with 24% total body surface area (TBSA) burns over a 3 week treatment period at Shriners Hospital for Children (Boston). During week 1 after the burn injury, there was an order of magnitude decrease in neutrophil cell count compared with the average range (shown with red dotted line) of a healthy volunteer (Fig. 5a). Moreover, we observed a 75% reduction in neutrophil velocity and a 50% reduction in directionality in neutrophils migrating toward a fMLP [100 nM] gradient (Fig. 5b,c). Data for LTB₄ was not available for this time-point. The number of cells accumulating towards fMLP spiked from below normal values to 15% above the normal healthy volunteer range at 2 weeks post-burn, which corresponded to a period when the patient was observed to have a fever. At 2 weeks post-burn, neutrophil velocity remained impaired in both fMLP and LTB₄ conditions (60% and 40% reduction respectively), but neutrophil directionality had been restored to the range of healthy volunteers (Fig. 5b,c). Three weeks post-burn, neutrophil cell counts to fMLP were lower than the average healthy volunteer count, whereas LTB₄ accumulation counts were in the normal range. Velocity and directionality were both restored to the normal range 3 weeks post-burn.

DISCUSSION

The first critical step in neutrophil function is the ability to correctly navigate to the site of injury or inflammation. If the neutrophil is lacking the ability to migrate to the area of infection, most subsequent markers of function are irrelevant and in some situation might even be detrimental to healthy surrounding tissues or organs. An assay to measure neutrophil chemotactic function is therefore the most important functional assay required in the clinical setting. To meet this need, we developed a novel microfluidic platform to measure neutrophil chemotaxis from a droplet of blood (2 μ L) reducing the time from blood collection to neutrophil migration assay from hours using traditional techniques, to just minutes.

Our device produces a stable linear chemoattractant gradient for the length of our experiment without the need for peripherals like an outside pressure source (i.e. syringe pump). Integration of an on-chip mechanical filtration comb in the novel platform presented, removes RBCs from actively migrating neutrophils and circumvents the need for cumbersome cell separation methods such as density gradients³⁴, positive selection³⁵, or negative selection³⁶, which are prone to introduce artifacts by activating neutrophils. For instance, previous work from our lab³⁷ and Sackmann *et al.*³⁸ utilized selections on the chip, for separating neutrophils from the whole blood sample, prior to the chemotaxis assay. After separation on selection surfaces, neutrophil migration occurred in buffer solution. Each of the selections (E, P, and L) are known to activate the neutrophils by engaging specific counterparts and therefore may alter *in vitro* chemotaxis measurements^{39–41}. In these conditions, any effect of serum on neutrophil chemotaxis was also removed. It is known that many factors in whole blood, including serum⁴² and platelets⁴³, affect neutrophil function. It is therefore advantageous to minimize sample processing to maintain the *in vivo*

microenvironment of the neutrophil when measuring variations in chemotaxis *in vitro* for clinical diagnostic purposes.

Critical for the performance of our assay, are the integrated microfluidic features which favor neutrophil migration through channels and selectively block the entrance of other blood cells based on size, deformability, or motility. The dimensions of the migration channels are optimized to selectively allow neutrophil chemotaxis and are generally too small for the migration of other leukocytes. For example, monocytes and lymphocytes, the next most frequent leukocytes in blood after neutrophils, are larger than the 3 μm height of the channels, and earlier studies in our lab have shown that these cells require channels that are at least $10 \times 10 \mu\text{m}$ for migration^{30,44}. The second selection mechanism to prevent other leukocytes from entering the migration channel of the device is the choice of chemoattractant. For example, fMLP is a neutrophil-specific chemoattractant and will not attract other leukocytes. In the case of chemokines shared by various types of leukocyte, e.g. LTB₄, neutrophils are two or more orders of magnitude more frequent in blood than other responsive cells e.g. monocytes or eosinophils. The combination of multiple selection mechanisms in the same device assures the device selectivity for chemotaxing neutrophils.

We validated the whole blood microfluidic platform by measuring neutrophil accumulation number, velocity and directionality in healthy donor samples. We established a healthy range of functional values for neutrophils migrating to both fMLP and LTB₄. We showed that there was minimal device-device variation and we were able to establish a consistent patient baseline for neutrophil functional variations over time. We also showed that neutrophils isolated from healthy donors have a high directional index and consistently follow the chemoattractant gradient towards the FCC. One interesting observation was the larger heterogeneity of capillary vs. venous blood neutrophils. One explanation for this situation may be that a significant fraction of the neutrophils obtained from a finger prick come from the margined pool inside capillaries⁴⁵, while the neutrophil population sampled from large veins is more homogenous. This possibility is supported by earlier observations of the higher neutrophil count (up to 12% higher) reported in capillary blood compared with venous blood sources^{29,46}. Other potential explanations include the transient activation of neutrophils by tissue factors released from the small injury inflicted by the lancet during blood collection, or activation after the brief contact with other cell types, such as endothelial cells⁴⁷ and pericytes⁴⁸ during blood collection. It is also important to note that the sample heterogeneity is smaller than the variations we measured between healthy volunteers, further conforming that our new approach is a robust and practical assay for human neutrophil chemotaxis studies.

The novel platform described will enable the study of neutrophil chemotaxis in infants or small mammals, where sample volume is limited, and is particularly useful for measuring transient neutrophil chemotactic deficiencies by facilitating repeated sampling over multiple time-points. We utilized the platform in the clinical setting to monitor a patient's neutrophil chemotactic function following a large surface area burn. We discovered a decrease in neutrophil chemotaxis velocity and directionality a week post-burn, which was restored to normal values 3 weeks after treatment. We also observed a spike in neutrophil counts when the patient had elevated temperature and was suspected to have an infection. These findings

demonstrate the potential of the whole blood device to be a useful tool for measuring transient deficiencies in neutrophil function in clinical settings. It can be utilized for patients with other conditions known to compromise immune function and where infection is prevalent, such as following major surgery. In the future, the migration channel cross-sectional area of the device could be optimized to measure chemotaxis of other leukocytes directly from whole blood, such as monocytes or lymphocytes. The incorporation of our device in a 12- or 24-wellplate facilitates the screening of multiple conditions simultaneously. This device also has the potential to facilitate the development of mediators of inflammation-resolution in order to treat burn and other inflammatory conditions.

METHODS

Microfluidic device fabrication

The microfluidic device to study neutrophil chemotaxis from a single droplet of whole blood is designed with three main components: Chemokine side chambers ($200 \times 200 \mu\text{m}$), a central whole-blood loading chamber, and migration channels containing RBC filtering regions (Fig. 1a). The filter for each migration channel consists of 10 short channels (length $\sim 75 \mu\text{m}$) connected horizontally through an approximately $200\text{-}\mu\text{m}$ -long channel to create 90° bending sections capable of trapping the RBCs in order to prevent them from dispersing into the rest of the migration channel (Fig. 1b). A gradient of the chemoattractant is established along the migration channels by diffusion between the chemoattractant chambers and the central loading chamber. All migration channels were designed to be $12 \mu\text{m}$ wide and $3 \mu\text{m}$ high to establish only a single column of RBCs for efficient trapping while allowing human neutrophils to easily penetrate through.

Microfluidic devices were produced by replica molding poly-dimethylsiloxane (Sylgard 184, Elsworth Adhesives, Wilmington, MA) on a master wafer fabricated using standard photolithographic technologies with Mylar photomasks (FineLine Imaging, Colorado Springs, CO). After curing for at least 3 hours in an oven set to 65°C , the PDMS layer covering the master was peeled off and holes were punched. First, the central loading chamber was punched using a 1.5 mm puncher and then a 5 mm puncher was used to cut out the entire donut-shaped device (Harris Uni-Core, Ted Pella Inc., Reading, Ca). A 12-well plate was then plasma treated along with the PDMS donut-shaped devices and bonded on a hot plate set to 85°C for 10 minutes.

Whole blood handling

Capillary blood ($50 \mu\text{L}$) was collected by pricking a finger of healthy volunteers. The blood was then pipetted into an eppendorf tube containing a mixed solution of HBSS media, heparin anti-coagulant ($1.65 \text{ USP}/50 \mu\text{L}$ of blood), and Hoescht stain ($10 \mu\text{L}$, $32.4 \mu\text{M}$). The eppendorf tube was then incubated for 10 minutes at 37°C and $5\% \text{ CO}_2$ to allow for proper staining of the nuclei. For venous blood samples, 10 mL of peripheral blood was drawn from a health volunteer into tubes containing 33 US Pherparin (Vacutainer, Becton Dickinson, Franklin Lakes, NJ). Afterwards, $50 \mu\text{L}$ of the blood was pipetted into media containing the same Hoescht stain concentration as previously described and incubated for 10 minutes at 37°C and $5\% \text{ CO}_2$. To compare out whole blood results with previous work, we also

isolated human neutrophils were isolated from whole blood using HetaSep followed by the EasySep Human Neutrophil Enrichment Kits (STEMCELL Technologies Inc. Vancouver, Canada) following the manufacturer's protocol. The final aliquots of neutrophils were re-suspended in 1X HBSS +0.2% human serum albumin (Sigma-Aldrich, St. Louis, MO) at a density of ~40,000 cells/ μ L and kept at 37°C until devices were properly primed.

Additionally, blood samples of 1 mL were collected from one burn patient admitted to Shriners' burn unit for children. The patient was a 16 y.o. male suffering from 24% total body surface area (TBSA) burn caused by a flame and flash gasoline accident. All patient samples were obtained with written informed consent, and through procedures approved by the Shriners Hospitals for Children and Massachusetts General Hospital Institutional Review Boards.

Microfluidic assay preparation

Immediately after bonding to the well plate, donut-shaped devices were filled with the chemoattractant solution of N-formyl-methionyl-leucyl-phenylalanine (fMLP) [100 nM] (Sigma-Aldrich, St. Louis, MO) or Leukotriene B₄ (LTB₄) (Caymen Chemicals, Ann Arbor, MI) [100 nM]. The chemoattractant solution also contained fibronectin [25 nM] (Sigma-Aldrich, St. Louis, MO) to promote neutrophil surface adhesion. The chemoattractant was pipetted into the whole blood loading chamber (WBLC) and directly around the circumference of the device. The glass bottom 12-well plate was then placed in a desiccator to de-gas for 15 minutes to ensure proper filling of the chambers while the PDMS surface was still hydrophilic from plasma treatment. Afterwards, the central whole-blood loading chamber and the outside region surrounding the donut were washed thoroughly with Phosphate Buffered Saline (PBS) in each well to wash away excess chemoattractant. The wells of the plate were then filled with RPMI 1640 media and allowed to sit for a period of 15 minutes to generate stable chemoattractant gradients. Finally, using a gel-loading tip, 2 μ L of whole blood was slowly pipetted into the central whole-blood loading chamber (Fig. 1a).

Chemotaxis imaging and measurements

Time-lapse imaging was performed on a Nikon Eclipse Ti microscope with 10–15X magnification and a biochamber heated to 37°C with 5% CO₂ and 80% humidity. Separate experiments to characterize the formation of gradients along the migration channels in the absence of cells were performed under similar temperature and gas conditions with Fluorescein sodium salt (molecular mass 376 Da) (Sigma-Aldrich, St. Louis, MO). For each experiment, at least 50 neutrophils were manually tracked. Directionality of primed neutrophils was quantified by counting the number of cells that followed the chemotactic gradient and turned at the bifurcation toward the chemoattractant chamber as opposed to the number of cells that exited the device to the peripheral region. Cell velocities were calculated using Image J (NIH) and data analysis with GraphPad Prism.

Biophysical simulations of RBC interactions

The channel geometries and initial RBC positions were then input into our custom-built finite-element software package PAK⁴⁹ and run on a desktop supercomputer consisting of

32 cores (Supermicro Super Server: 4× Eight-Core Intel Xeon Processor 2.70 GHz; 512 GB total memory). Biophysical modeling of chemoattractant diffusion in the device was performed using COMSOL Multiphysics software. We simulated the granular flow of RBCs through small channels and focused specifically on how a group of 10 RBCs that have entered the microchannels from the main reservoir of the device, traverse a 90° turn (Fig. 2a–d). This movement is a result of the mutual interaction of many RBCs in the whole blood loading chamber, pushing the RBCs at the periphery to enter the connected microchannels. To simulate this force, we have assumed that the top-most RBC (marked with a red outline experiences an external force (equal to 1/50 g, the equivalent of a stack of twelve RBCs with 5% higher density than that of media pushing one RBC into the channels) in the y-direction, whereas the other RBCs below it have no externally applied forces.

Acknowledgments

Support from the National Institutes of Health (grants GM092804, DE019938). We also thank Martha Lydon at the Shriners Hospitals for Children for help collecting patient blood samples.

References

1. Hansson GK, Robertson AK, Soderberg-Naucler C. Inflammation and atherosclerosis. *Annu Rev Pathol.* 2006; 1:297–329. [PubMed: 18039117]
2. Butler KL, et al. Burn injury reduces neutrophil directional migration speed in microfluidic devices. *PLoS One.* 2010; 5:e11921. [PubMed: 20689600]
3. Murray CK, et al. Evaluation of white blood cell count, neutrophil percentage, and elevated temperature as predictors of bloodstream infection in burn patients. *Arch Surg.* 2007; 142:639–642. [PubMed: 17638801]
4. Lavrentieva A, et al. Inflammatory markers in patients with severe burn injury. What is the best indicator of sepsis? *Burns.* 2007; 33:189–194. [PubMed: 17215085]
5. Bogomolski-Yahalom V, Matzner Y. Disorders of neutrophil function. *Blood Rev.* 1995; 9:183–190. [PubMed: 8563520]
6. Matzner Y. Neutrophil function studies in clinical medicine. *Transfus Med Rev.* 1987; 1:171–181. [PubMed: 2980276]
7. Dinauer MC. Disorders of neutrophil function: An overview. *Methods Mol Biol.* 2007; 412:489–504. [PubMed: 18453130]
8. Stepanovic V, Wessels D, Goldman FD, Geiger J, Soll DR. The chemotaxis defect of Shwachman-Diamond Syndrome leukocytes. *Cell Motil Cytoskeleton.* 2004; 57:158–174. [PubMed: 14743349]
9. Babcock GF. Predictive medicine: Severe trauma and burns. *Cytometry B Clin Cytom.* 2003; 53:48–53. [PubMed: 12717691]
10. Buffone V, Meakins JL, Christou NV. Neutrophil function in surgical patients. Relationship to adequate bacterial defenses. *Arch Surg.* 1984; 119:39–43. [PubMed: 6689872]
11. Wierusz-Wysocka B, et al. Evidence of polymorphonuclear neutrophils (PMN) activation in patients with insulin-dependent diabetes mellitus. *J Leukoc Biol.* 1987; 42:519–523. [PubMed: 2824647]
12. Kantarci A, Oyaizu K, Van Dyke TE. Neutrophil-mediated tissue injury in periodontal disease pathogenesis: Findings from localized aggressive periodontitis. *J Periodontol.* 2003; 74:66–75. [PubMed: 12593599]
13. Van Dyke TE, Horoszewicz HU, Cianciola LJ, Genco RJ. Neutrophil chemotaxis dysfunction in human periodontitis. *Infect Immun.* 1980; 27:124–132. [PubMed: 7358424]
14. Kobasa D, et al. Enhanced virulence of influenza A viruses with the haemagglutinin of the 1918 pandemic virus. *Nature.* 2004; 431:703–707. [PubMed: 15470432]

15. Bale JF Jr, Kern ER, Overall JC Jr, Baringer JR. Impaired migratory and chemotactic activity of neutrophils during murine cytomegalovirus infection. *J Infect Dis.* 1983; 148:518–525. [PubMed: 6311912]
16. Martin LS, Spira TJ, Orloff SL, Holman RC. Comparison of methods for assessing chemotaxis of monocytes and polymorphonuclear leukocytes isolated from patients with AIDS or AIDS-related conditions. *J Leukoc Biol.* 1988; 44:361–366. [PubMed: 2846727]
17. Heit B, et al. HIV and other lentiviral infections cause defects in neutrophil chemotaxis, recruitment, and cell structure: Immunorestorative effects of granulocyte-macrophage colony-stimulating factor. *J Immunol.* 2006; 177:6405–6414. [PubMed: 17056572]
18. Gartner EM, Anderson R. An *in vitro* assessment of cellular and humoral immune function in pulmonary tuberculosis: Correction of defective neutrophil motility by ascorbate, levamisole, metoprolol and propranolol. *Clin Exp Immunol.* 1980; 40:327–335. [PubMed: 7002387]
19. Rivkin I, Rosenblatt J, Becker EL. The role of cyclic AMP in the chemotactic responsiveness and spontaneous motility of rabbit peritoneal neutrophils. The inhibition of neutrophil movement and the elevation of cyclic AMP levels by catecholamines, prostaglandins, theophylline and cholera toxin. *J Immunol.* 1975; 115:1126–1134. [PubMed: 170335]
20. Leoratti FM, et al. Neutrophil paralysis in *Plasmodium vivax* malaria. *PLoS Negl Trop Dis.* 2012; 6:e1710. [PubMed: 22745844]
21. Leblanc AK, Leblanc CJ, Rohrbach BW, Kania SA. Serial evaluation of neutrophil function in tumour-bearing dogs undergoing chemotherapy. *Vet Comp Oncol.* 2013 Epub ahead of print.
22. Clapperton M, McMurray J, Fisher AC, Dargie HJ. The effect of angiotensin-converting enzyme inhibitors on human neutrophil chemotaxis *in vitro*. *Br J Clin Pharmacol.* 1994; 38:53–56. [PubMed: 7946937]
23. Mikawa K, Akamatsu H, Nishina K, Uesugi T, Niwa Y. The effects of pentazocine, buprenorphine and butorphanol on human neutrophil functions. *Acta Anaesthesiol Scand.* 2006; 50:643–644. [PubMed: 16643251]
24. Nishina K, et al. The inhibitory effects of thiopental, midazolam, and ketamine on human neutrophil functions. *Anesth Analg.* 1998; 86:159–165. [PubMed: 9428872]
25. Mikawa K, Akamatsu H, Nishina K, Niwa Y. Effects of pirenzepine, omeprazole, lansoprazole, and rabeprazole on human neutrophil functions. *Can J Anaesth.* 2001; 48:421–422. [PubMed: 11339790]
26. Roilides E, Walsh TJ, Rubin M, Venzon D, Pizzo PA. Effects of antifungal agents on the function of human neutrophils *in vitro*. *Antimicrob Agents Chemother.* 1990; 34:196–201. [PubMed: 2158275]
27. Boner A, Zeligs BJ, Bellanti JA. Chemotactic responses of various differentional stages of neutrophils from human cord and adult blood. *Infect Immun.* 1982; 35:921–928. [PubMed: 7068221]
28. Kojic N, et al. A 3-D model of ligand transport in a deforming extracellular space. *Biophys J.* 2010; 99:3517–3525. [PubMed: 21112275]
29. Kojic N, Kojic A, Kojic M. Numerical determination of the solvent diffusion coefficient in a concentrated polymer solution. *Commun Numer Methods Eng.* 2006; 22:1003–1013.
30. Jones CN, et al. Microfluidic chambers for monitoring leukocyte trafficking and humanized nanopresolving medicines interactions. *Proc Natl Acad Sci USA.* 2012; 109:20560–20565. [PubMed: 23185003]
31. Heit B, Tavener S, Raharjo E, Kubes P. An intracellular signaling hierarchy determines direction of migration in opposing chemotactic gradients. *J Cell Biol.* 2002; 159:91–102. [PubMed: 12370241]
32. Malawista SE, de Boisfleury Chevance A, van Damme J, Serhan CN. Tonic inhibition of chemotaxis in human plasma. *Proc Natl Acad Sci USA.* 2008; 105:17949–17954. [PubMed: 18997012]
33. Everitt EA, Malik AB, Hendey B. Fibronectin enhances the migration rate of human neutrophils *in vitro*. *J Leukoc Biol.* 1996; 60:199–206. [PubMed: 8773581]
34. Nauseef WM. Isolation of human neutrophils from venous blood. *Methods Mol Biol.* 2007; 412:15–20. [PubMed: 18453102]

35. Lyons PA, et al. Microarray analysis of human leucocyte subsets: The advantages of positive selection and rapid purification. *BMC Genomics*. 2007; 8:64. [PubMed: 17338817]
36. Hasenberg M, et al. Rapid immunomagnetic negative enrichment of neutrophil granulocytes from murine bone marrow for functional studies *in vitro* and *in vivo*. *PLoS One*. 2011; 6:e17314. [PubMed: 21383835]
37. Kasuga K, et al. Rapid appearance of resolvin precursors in inflammatory exudates: Novel mechanisms in resolution. *J Immunol*. 2008; 181:8677–8687. [PubMed: 19050288]
38. Sackmann EK, et al. Microfluidic kit-on-a-lid: A versatile platform for neutrophil chemotaxis assays. *Blood*. 2012; 120:e45–53. [PubMed: 22915642]
39. Smolen JE, et al. L-selectin signaling of neutrophil adhesion and degranulation involves p38 mitogen-activated protein kinase. *J Biol Chem*. 2000; 275:15876–15884. [PubMed: 10748078]
40. Blanks JE, Moll T, Eytner R, Vestweber D. Stimulation of P-selectin glycoprotein ligand-1 on mouse neutrophils activates beta 2-integrin mediated cell attachment to ICAM-1. *Eur J Immunol*. 1998; 28:433–443. [PubMed: 9521050]
41. Simon SI, Hu Y, Vestweber D, Smith CW. Neutrophil tethering on E-selectin activates beta 2 integrin binding to ICAM-1 through a mitogen-activated protein kinase signal transduction pathway. *J Immunol*. 2000; 164:4348–4358. [PubMed: 10754335]
42. Mankovich AR, Lee CY, Heinrich V. Differential effects of serum heat treatment on chemotaxis and phagocytosis by human neutrophils. *PLoS One*. 2013; 8:e54735. [PubMed: 23349959]
43. Palabrica T, et al. Leukocyte accumulation promoting fibrin deposition is mediated *in vivo* by P-selectin on adherent platelets. *Nature*. 1992; 359:848–851. [PubMed: 1279433]
44. Hoerning A, et al. Subsets of human CD4(+) regulatory T cells express the peripheral homing receptor CXCR3. *Eur J Immunol*. 2011; 41:2291–2302. [PubMed: 21538345]
45. Summers C, et al. Neutrophil kinetics in health and disease. *Trends Immunol*. 2010; 31:318–324. [PubMed: 20620114]
46. Peevy KJ, Grant PH, Hoff CJ. Capillary venous differences in neonatal neutrophil values. *Am J Dis Child*. 1982; 136:357–358. [PubMed: 7072669]
47. Yuan SY, Shen Q, Rigor RR, Wu MH. Neutrophil transmigration, focal adhesion kinase and endothelial barrier function. *Microvasc Res*. 2012; 83:82–88. [PubMed: 21864543]
48. Stark K, et al. Capillary and arteriolar pericytes attract innate leukocytes exiting through venules and ‘instruct’ them with pattern-recognition and motility programs. *Nat Immunol*. 2013; 14:41–51. [PubMed: 23179077]
49. Kojic, M.; Filipovic, N.; Slavkovic, R.; Zivkovic, M.; Grujoric, N. PAK-FS-Finite Element Program for Fluid Flow and Fluid-Solid Interaction. University of Kragujevac and R&D Center for Bioengineering; Kragujevac, Serbia: 2010.

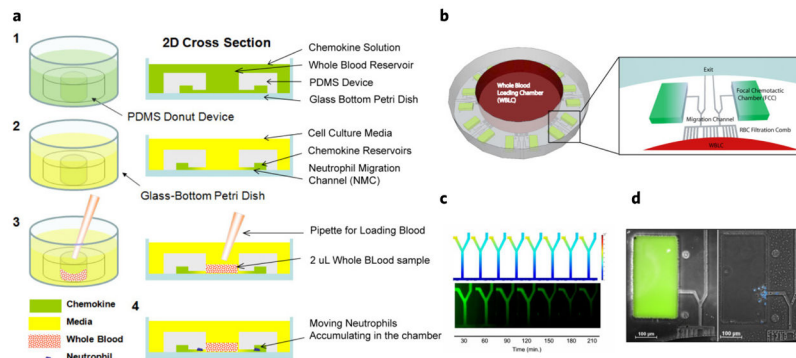


Figure 1. Characterization of whole blood (WB) microfluidic device. **(a)** Diagram of chemotaxis assay setup. 1. Chemoattractant is pipetted into whole blood loading chamber and around the perimeter of the device. Device is placed in desiccator under vacuum and the focal chemotactic chamber is primed. 2. Device is washed and submerged in media. The gradient is formed between the focal chemotactic chamber and the whole blood loading chamber along the migration channel. 3. 2 μ L of whole blood is loaded into the device. 4. Neutrophils migrate out of whole blood along chemoattractant gradient and accumulate in the focal chemotactic chamber. **(b)** A three-dimensional schematic of donut-shaped whole blood device. Sixteen FCCs surround each WBLC. Chemoattractant (green) is primed into the device and after washing, the chemoattractant only remains in the FCC, and a linear gradient is formed along the migration channel toward the FCC. A RBC filtration comb, upstream of the migration channel, blocks RBC contamination of device while allowing the active migration on neutrophils out of whole blood. The bifurcation in the device allows quantification of directionality in neutrophils by comparing cells that correctly follow the chemoattractant gradient to the FCC with those that exit the device. **(c)** COMSOL finite element modeling of chemoattractant gradient over the duration of the experiment. The gradient is reduced by 5% after 210 min. **(d)** Image of experimental chemoattractant gradient (green) with FITC-conjugated dextran with a similar MW of a standard chemoattractant (fMLP) (left). Bright field (BF) image of neutrophils migrating along chemoattractant gradient and cell accumulation in the FCC (right).

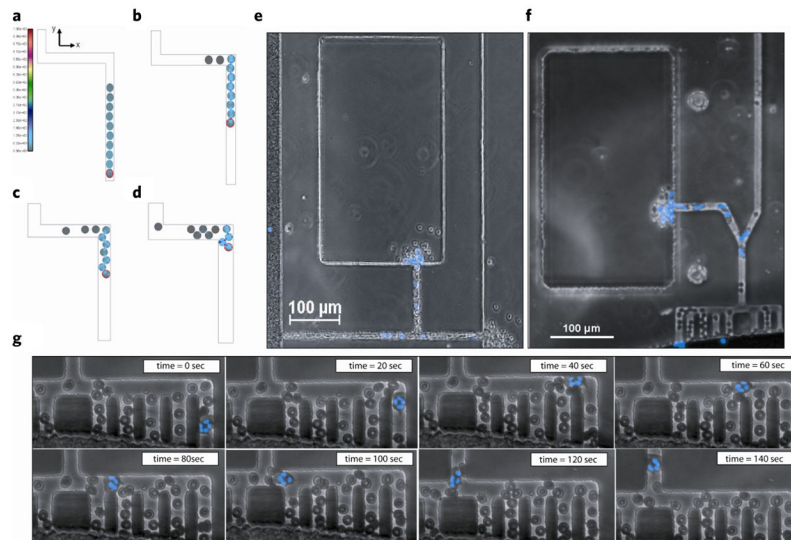


Figure 2. Red blood cell filtration. Numerical modeling of RBC arrest in various channel geometries. Displayed are internal stresses for each of the 10 RBCs. The RBC with the red outline represents the RBC on which an external force (equal to $1/50$ g in the y-direction) is applied in order to move the RBCs in front of it. (a) Initial configuration of 10 RBCs in a 9-micron wide channel (RBC diameter is 7.5 microns). Scale bar indicates stress values. (b) Final, steady-state configuration inside the 9-micron channel showing only two RBCs have successfully passed the corner. (c) 12-micron channel showing three RBCs have moved through the corner (initial RBC configuration same as in A). (d) 14-micron channel showing most RBCs have passed the corner (initial RBC configuration same as in A). (e) BF image of a device without a RBC filtration comb. RBCs are seen to clog the migration channel and contaminate the FCC and exit (see arrows). (f) The incorporation of a RBC filtration comb upstream of the migration channel significantly reduces RBC contamination in the FCC by 63% and eliminates RBCs at the channel exit. (g) Few RBCs are seen in the migration channel and neutrophils are able to actively migrate past these RBCs (see Movie 1).

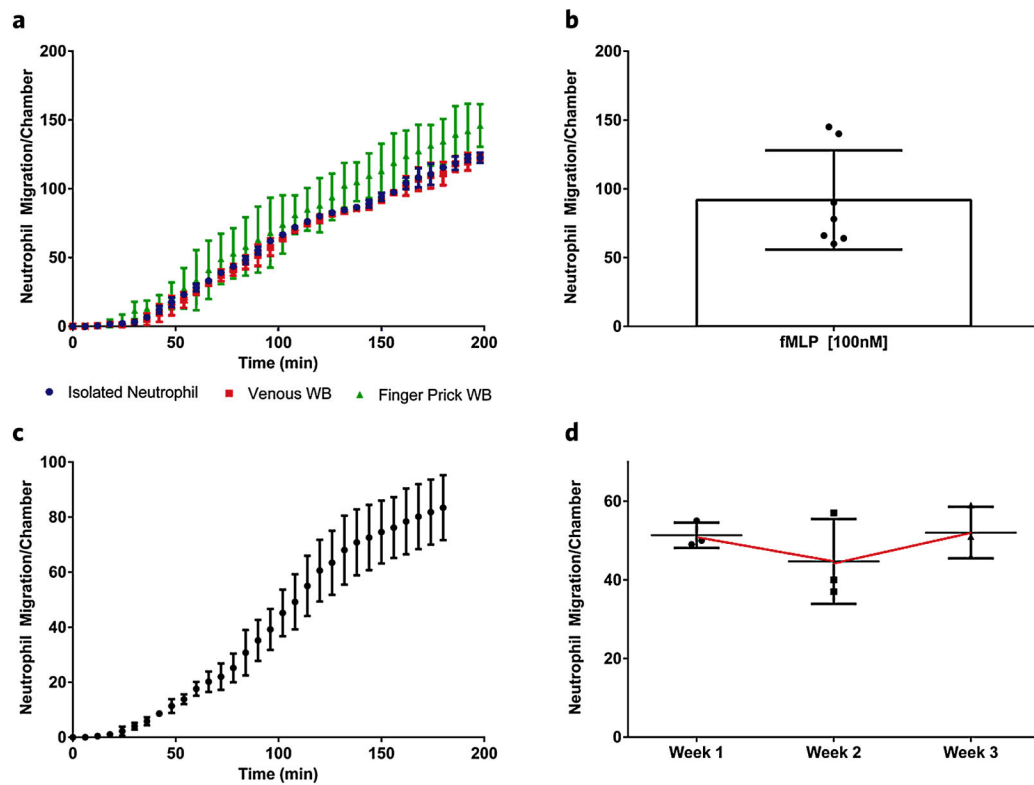


Figure 3.

Validation of whole blood platform. **(a)** Neutrophil migration counts are compared between venous and finger prick blood sources and isolated neutrophils. A similar delay time, accumulation rate and final cell count are observed in all three conditions migrating to fMLP [100 nM]. Graphs correspond to average cell counts in all FCCs ($n = 16$). **(b)** Neutrophil migration counts per chamber are compared for 7 healthy volunteers. **(c)** Average neutrophil migration counts to fMLP [100 nM] in 6 separate whole blood devices. **(d)** Baseline for neutrophil migration in healthy donor to fMLP [100 nM] over a 3 week time course.

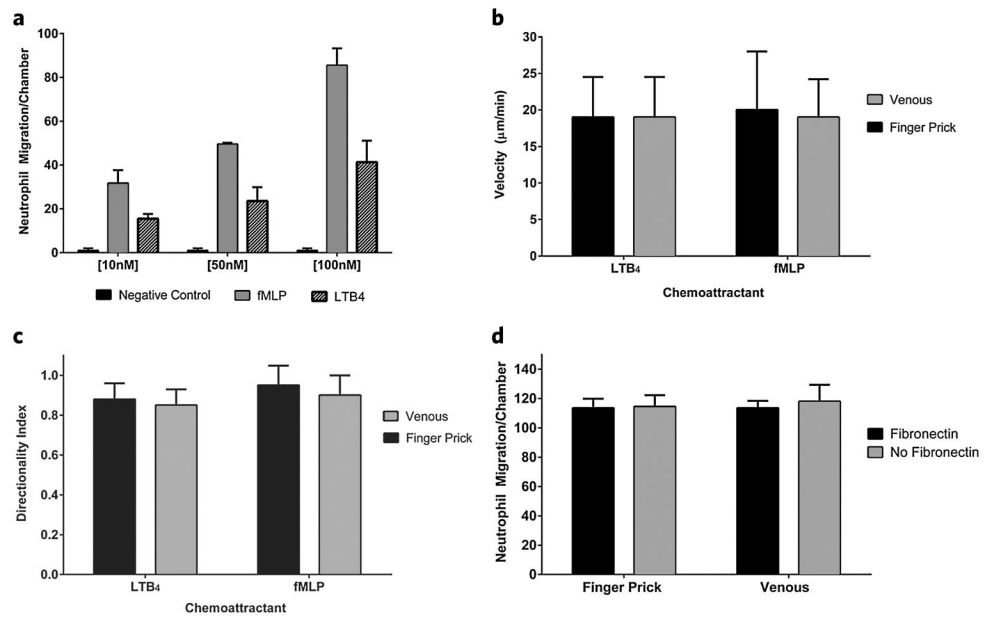


Figure 4.

Comparison of LTB₄ and fMLP. (a) Dose–response of LTB₄ and fMLP as a chemoattractant to neutrophils migrating out of whole blood. Graphs correspond to average cell counts in all FCCs (n = 16). Cells do not migrate in absence of chemoattractant gradient. (b) Velocity [µm/min] of neutrophils migrating to LTB₄ compared with fMLP. (c) Directionality of neutrophils migrating to LTB₄ compared with fMLP. (d) Neutrophil counts migrating to fMLP are compared with and without the extracellular matrix protein fibronectin [100 nM] added to the chemoattractant solution.

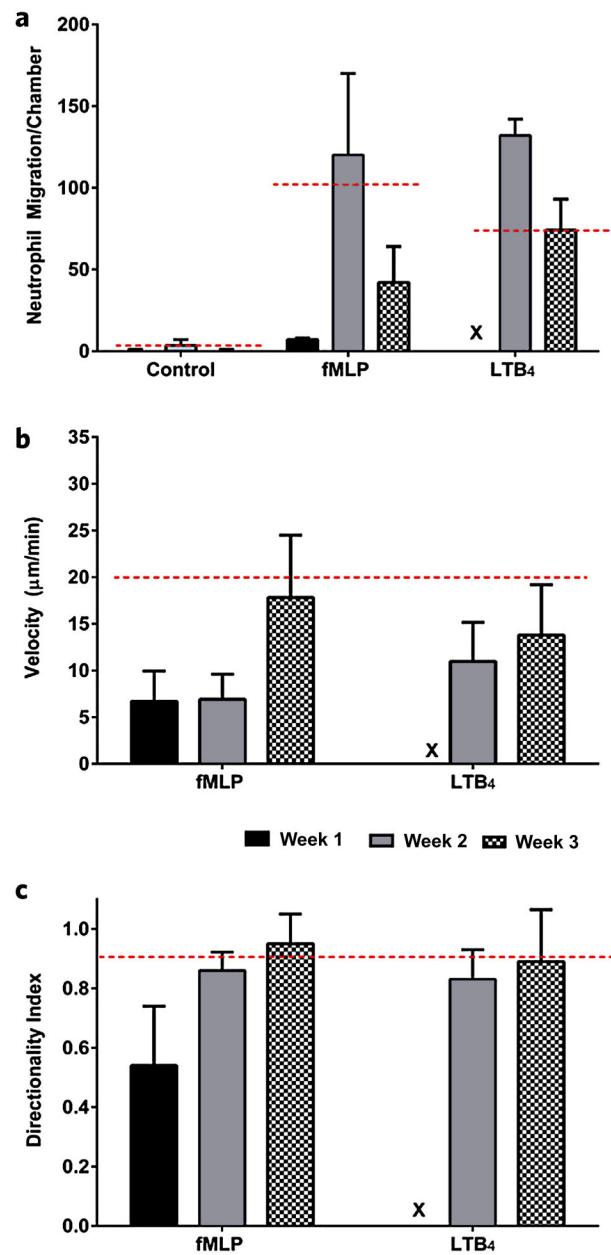


Figure 5. Burn patient neutrophil chemotactic impairment. Whole blood samples from a 16 y.o. patient with 24% TBSA burns were taken over a 3 week treatment period. **(a)** Neutrophil migration counts in FCC of neutrophils migrating in the absence of a chemoattractant gradient (media only), to fMLP [100 nM] and LTB₄ [100 nM]. **(b)** Velocity [$\mu\text{m}/\text{min}$] of neutrophils migrating to LTB₄ compared with fMLP. **(c)** Directionality of neutrophils migrating to LTB₄ compared with fMLP. All graphs correspond to average cell counts in all FCCs ($n = 16$).